

# Investigation of thermo-optic effect and multi-reflector tunable filter/multiplexer in SOI waveguides

Vittorio M. N. Passaro, Francesca Magno

Politecnico di Bari, Dipartimento di Elettrotecnica ed Elettronica,  
via Edoardo Orabona n.4, 70125 Bari, Italy  
[passaro@deemail.poliba.it](mailto:passaro@deemail.poliba.it)

Andrei V. Tsarev

Institute of Semiconductor Physics, Siberian Branch Russian Academy of Sciences  
Prospect Lavrenteva, 13, Novosibirsk, 630090, Russia  
[tsarev@thermo.isp.nsc.ru](mailto:tsarev@thermo.isp.nsc.ru)

**Abstract:** The paper presents an analysis of thermo-optic phase shifters in silicon-on-insulator (SOI) waveguide structures. It gives recommendations to provide high tuning characteristics at minimum power requirements. Then, this analysis is applied to the description of a novel type of reconfigurable optical add/drop multiplexer (ROADM) utilizing multi-reflector (MR) beam expanders and thermo-optic tuning in SOI structures. It is intended for use in high dense wavelength-division-multiplexing (HDWDM) flexible fiber-optic networks having multi-hundreds wavelength channels and advanced ITU grids (12.5 GHz, 25 GHz, 50 GHz).

©2005 Optical Society of America

**OCIS codes:** 060.1810 Couplers, switches, and multiplexers; 130.0130 Integrated optics; 130.3120 Integrated optics devices; 130.5990 Semiconductors; 160.6840 Thermo-optical materials

---

## References and Links

1. G. T. Reed and A. P. Knights, *Silicon Photonics* (Wiley, 2004).
2. Shyh-Lin Tsao, Jiang-H. Tien, and Chun-Wei Tsai, "Simulations on an SOI Grating-Based Optical Add/Drop Multiplexer," *IEEE J. of Sel. Top. in Quantum Electron.* **8**, 1277-1284 (2002).
3. P. Dainesi, A. Küng, M. Chabloz, A. Lagos, Ph. Flückiger, A. Ionescu, P. Fazan, M. Declercq, Ph. Renaud, and Ph. Robert, "CMOS Compatible Fully Integrated Mach-Zehnder Interferometer in SOI Technology," *IEEE Photon. Technol. Lett.* **12**, 660-662 (2000).
4. W. Bogaerts, R. Baets, P. Dumon, V. Wiaux, S. Beckx, D. Taillaert, B. Luyssaert, J. Van Campenhout, P. Bienstman, and D. Van Thourhout, "Nanophotonic Waveguides in Silicon-on-Insulator Fabricated With CMOS Technology," *J. Lightwave Technol.* **23**, 401-412 (2005).
5. G. K. Ho, R. Abdolvand, and F. Ayazi, "Through-Support-Coupled Micromechanical Filter Array", 17th IEEE Int. Conf. on MEMS, 769-772 (2004).
6. G. Cocorullo, F. G. Della Corte, M. Iodice, I. Rendina, and P. M. Sarro, "A Temperature All-Silicon Micro-Sensor Based on the Thermo-optic Effect," *IEEE Trans. on Electron Devices* **44**, 766-774 (1997).
7. M. Harjanne, M. Kapulainen, T. Aalto, and P. Heimala, "Sub- $\mu$ s Switching Time in Silicon-on-Insulator Mach-Zehnder Thermo-optic Switch," *IEEE Photon. Technol. Lett.* **16**, 2039-2041 (2004).
8. M. W. Geis, S. J. Spector, R. C. Williamson, and T. M. Lyszczarz, "Submicrosecond Submilliwatt Silicon-on-Insulator Thermo-optic Switch," *IEEE Photon. Technol. Lett.* **16**, 2514-2516 (2004).
9. A.V. Tsarev, "Tunable optical filters," United States Patent No. US20040247221 A1, December 9 (2004).
10. A.V. Tsarev, "Beam-expanding device," United States Patent No. 6,836,601, December 28 (2004).
11. A.V. Tsarev, "Optical beam expander," Russian Federation Patent No. 2183337, Bulletin No. 16, June 10 (2002).
12. FEMLAB 3.0 by Comsol AB, Sweden, trial license (2004).
13. R. L. Espinola, M.-C. Tsai, J. T. Yardley, and R. M. Osgood, Jr., "Fast and Low-Power Thermo-optic Switch on Thin Silicon-on-Insulator," *IEEE Photon. Technol. Lett.* **15**, 1366-1368 (2003).
14. U. Fischer, T. Zinke, B. Schuppert and K. Petermann, "Single-mode optical switches based on SOI waveguides with large cross-section," *Electron. Letters* **30**, 406-408 (1994).
15. OptiFDTD 3.0 by Optiwave Corporation, Canada/USA, trial license (2003).

16. H. Yoda, K. Shiraishi, Y. Hiratani, and O. Hanaizumi, "a-Si:H/SiO<sub>2</sub> multilayer films fabricated by radio-frequency magnetron sputtering for optical filters," *Appl. Opt.* **43**, 3548-3554 (2004).
17. G. Cocorullo, F.G. Della Corte, R. De Rosa, I. Rendina, A. Rubino, and E. Terzini, "Amorphous Silicon-Based Guided-Wave Passive and Active Devices for Silicon Integrated Optoelectronics," *IEEE J. of Sel. Top. in Quantum Electron.* **4**, 997-1002 (1998).

## 1. Introduction

Silicon-on-insulator (SOI) waveguide structures are very promising for the realization of dense photonic integrated circuits and firmly established within optoelectronic industry, being used as the basis for sophisticated components such as multiplexer, demultiplexer, optical attenuators and add-drop filters [1-2]. They are characterized by small optical losses over communication wavelengths and fully compatible with CMOS technology and micromechanical devices [3-5]. Silicon is available in large size, good quality and low price, and its technology is highly developed.

A typical SOI waveguide has a silicon core (refractive index  $n \sim 3.5$ ) and a silica cladding ( $n \sim 1.5$ ). Therefore there is a very high index contrast, enabling high confinement of the optical modes. SOI waveguides can be single-mode even with large dimensions using a rib structure (see Fig. 1), since the bottom slab waveguide offers an "escape path" for the higher order modes.

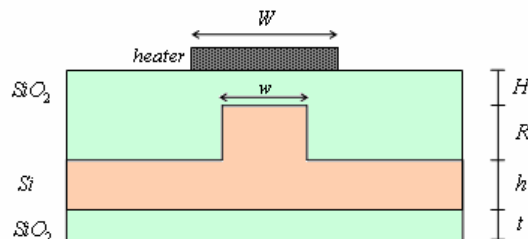


Fig. 1. Schematic diagram of the SOI waveguide cross section.

An attractive way to modulate the refractive index in SOI waveguides is the thermo-optic effect, allowing low transmission loss, low cost, high stability, low power consumption and very large scale of integration. Silicon doesn't possess a linear electro-optic effect, but has a very high thermo-optic coefficient  $dn/dT$  ( $1.86 \cdot 10^{-4} \text{ K}^{-1}$  at  $\lambda = 1.55 \text{ }\mu\text{m}$ ), compared with the most commonly used semiconductors and optical materials [6]. This high thermo-optic constant allows low power and fast time response to be achieved [7-8]. However, in literature there are no papers where a theoretical optimization of the heated SOI structures is extensively presented.

We have simulated various SOI rib waveguides to be used for low power, high speed thermo-optic devices, such as modulators and reconfigurable optical add/drop multiplexers (ROADMs). In fact, optical switches, tunable optical filters (TOF) and ROADMs are key components in optical communication systems. In this paper we have focused on achieving optimized switching characteristics, i.e., fast response and low power performance, varying the dimensions of the SOI waveguide and heater.

Then, this thermal investigation has been applied to the analysis of a new perspective type of ROADM, based on multi-reflector (MR) filtering technology [9]. It accomplishes filtering by spatially expanding the optical beam through a patented MR-beam expander (BE) [10-11], then tuning and filtering the desired wavelength through a set of tunable channel waveguides and finally by constructively interfering multiple sub-beams, combined in the output strip waveguide by another beam expander. Multi-reflector technology provides possibility of development tunable devices (TOF and ROADM) for high dense wavelength-division-multiplexing (HDWDM) fiber-optic networks that utilize advanced ITU grids (12.5 GHz, 25 GHz, 50 GHz). In principle devices can be developed on different materials (silicon, polymer,

etc.), allowing partial reflector manufacturing, optical phase tunability and low optical losses in single-mode waveguides.

## 2. Numerical results of SOI waveguide heating

We have simulated a series of SOI rib waveguides by using the 2D finite element method (FEM) [12]. A schematic diagram of the waveguide cross section is sketched in Fig. 1. The thickness  $t$  of the silica bottom layer was set at  $1.3\ \mu\text{m}$  for all the structures. The other sizes as well as results of simulations are summarised in Table 1 for quasi-TE polarized waveguides. The structures named with the same number but different letter correspond to identical waveguides where only the distance  $H$  of the heater and/or the heater width  $W$  was changed. In the following Table 2 the quasi-TM polarized cases are summarized, only slightly different from quasi-TE results, the difference being always very small (relative change less than 0.26%), i.e., negligible for practical uses. These simulations confirm the isotropic behaviour of these SOI rib structures, even with small cross section (sizes smaller than the wavelength,  $\lambda = 1.55\mu\text{m}$ ). Then, we have same thermo-optic effect with polarization, useful to select efficient thermo-optic switches or other thermo-optic devices. It is important to note that all the investigated structures are single mode (for both polarizations), and structures 2 and 3a are polarization-insensitive too.

Table 1. Waveguide geometric dimensions, thermo-optic coefficient, switching power and cut-off frequency (TE).

N.	$W$ [ $\mu\text{m}$ ]	$h$ [ $\mu\text{m}$ ]	$R$ [ $\mu\text{m}$ ]	$w$ [ $\mu\text{m}$ ]	$H$ [ $\mu\text{m}$ ]	$dn_{\text{eff}}/dT$ [ $\text{K}^{-1}$ ]	$P_{\pi}$ [mW]	$f_{\text{cut-off}}$ [kHz]	$f_{\text{cut-off}}/P_{\pi}$
3a	3	0.36	0.64	0.52	0.1	$1.429 \cdot 10^{-4}$	17.39	16.76	0.96377
3b	3	0.36	0.64	0.52	0.01	$1.654 \cdot 10^{-4}$	15.02	18.25	1.21505
3c	3	0.36	0.64	0.52	0.5	$1.093 \cdot 10^{-4}$	22.73	12.29	0.54069
2	3	0.48	0.78	0.8	0.1	$1.507 \cdot 10^{-4}$	16.50	12.03	0.72909
1a	3	0.6	0.9	1.1	1	$9.463 \cdot 10^{-5}$	26.29	5.95	0.22632
1b	3	0.6	0.9	1.1	0.5	$1.191 \cdot 10^{-4}$	20.90	7.43	0.35550
1c	3	0.6	0.9	1.1	0.4	$1.257 \cdot 10^{-4}$	19.79	7.82	0.39515
1d	3	0.6	0.9	1.1	0.1	$1.568 \cdot 10^{-4}$	15.87	9.29	0.58538
1e	3	0.6	0.9	1.1	0.01	$1.759 \cdot 10^{-4}$	14.14	9.84	0.69590
7	3	1.2	1.6	2	0.1	$1.564 \cdot 10^{-4}$	15.97	3.79	0.23732
4	3	1.8	2.7	3	0.1	$1.575 \cdot 10^{-4}$	15.90	1.99	0.12516
5	3	3.0	4.5	5	0.1	$1.496 \cdot 10^{-4}$	16.80	0.96	0.05714
6	3	4.8	5.6	8	0.1	$1.375 \cdot 10^{-4}$	18.37	0.56	0.03048

N.	$W$ [ $\mu\text{m}$ ]	$h$ [ $\mu\text{m}$ ]	$R$ [ $\mu\text{m}$ ]	$w$ [ $\mu\text{m}$ ]	$H$ [ $\mu\text{m}$ ]	$dn_{\text{eff}}/dT$ [ $\text{K}^{-1}$ ]	$P_{\pi}$ [mW]	$f_{\text{cut-off}}$ [kHz]	$f_{\text{cut-off}}/P_{\pi}$
3a	0.52	0.36	0.64	0.52	0.1	$1.246 \cdot 10^{-4}$	3.56	3.48	0.97753
3b	0.52	0.36	0.64	0.52	0.01	$1.639 \cdot 10^{-4}$	2.71	3.79	1.39852
2	0.8	0.48	0.78	0.8	0.1	$1.414 \cdot 10^{-4}$	4.78	3.67	0.76778
1b	1.1	0.6	0.9	1.1	0.5	$1.046 \cdot 10^{-4}$	8.84	3.02	0.34163
1d	1.1	0.6	0.9	1.1	0.1	$1.507 \cdot 10^{-4}$	6.14	3.78	0.61564
1e	1.1	0.6	0.9	1.1	0.01	$1.754 \cdot 10^{-4}$	5.28	2.82	0.53410
7	2	1.2	1.6	2	0.1	$1.532 \cdot 10^{-4}$	10.93	2.63	0.24062
5	5	3.0	4.5	5	0.1	$1.600 \cdot 10^{-4}$	26.00	1.51	0.05808
6	8	4.8	5.6	8	0.1	$1.604 \cdot 10^{-4}$	41.39	1.35	0.03262

First we have studied the optical propagation in the rib waveguides, using  $n = 3.478$  for silicon and  $n = 1.447$  for silica refractive index, respectively. Then we have analysed the same structures considering the effect induced by a top aluminium heater,  $0.5\mu\text{m}$  thick, lying on the structure at different distances from the rib. We have used the following values of thermal conductivity, density and specific heat capacity,  $k_{\text{Si}} = 163\ \text{W/m}\cdot\text{K}$ ,  $\rho_{\text{Si}} = 2.330\ \text{g/cm}^3$ ,  $C_{\text{Si}} = 0.703\ \text{J/g}\cdot\text{K}$  for silicon, and  $k_{\text{SiO}_2} = 1.38\ \text{W/m}\cdot\text{K}$ ,  $\rho_{\text{SiO}_2} = 2.203\ \text{g/cm}^3$ ,  $C_{\text{SiO}_2} = 0.703\ \text{J/g}\cdot\text{K}$  for

silica layers, respectively. The heat conduction equation has been solved by the 2D FEM as a boundary-value problem, by imposing the temperature at each heater edge.

Table 2. Waveguide geometric dimensions, thermo-optic coefficient, switching power and cut-off frequency (TM).

N.	$W$ [ $\mu\text{m}$ ]	$h$ [ $\mu\text{m}$ ]	$R$ [ $\mu\text{m}$ ]	$w$ [ $\mu\text{m}$ ]	$H$ [ $\mu\text{m}$ ]	$dn_{eff}/dT$ [ $\text{K}^{-1}$ ]	$P_\pi$ [mW]	$f_{cut-off}$ [kHz]	$f_{cut-off}$ / $P_\pi$
3b	3	0.36	0.64	0.52	0.01	$1.650 \cdot 10^{-4}$	15.05	18.24	1.21196
1b	3	0.6	0.9	1.1	0.5	$1.189 \cdot 10^{-4}$	20.93	7.43	0.35499
1c	3	0.6	0.9	1.1	0.4	$1.261 \cdot 10^{-4}$	19.73	7.82	0.39635
1e	3	0.6	0.9	1.1	0.01	$1.761 \cdot 10^{-4}$	14.12	9.84	0.69688
4	3	1.8	2.7	3	0.1	$1.571 \cdot 10^{-4}$	15.94	1.99	0.12484
5	3	3.0	4.5	5	0.1	$1.500 \cdot 10^{-4}$	16.75	0.96	0.05731
1e	1.1	0.6	0.9	1.1	0.01	$1.757 \cdot 10^{-4}$	5.27	2.82	0.53510

Thus, we have simulated different temperatures of the heater and observed for each one the relevant temperature distribution in the waveguide layers. Then, the refractive index change has been calculated for each layer of the structure and for each temperature by using the bulk thermo-optic coefficients,  $1.86 \cdot 10^{-4} \text{ K}^{-1}$  (silicon) and  $1.0 \cdot 10^{-5} \text{ K}^{-1}$  (silica), at a wavelength of  $1.55 \mu\text{m}$ . Using the new refractive indices, we have performed again the mode analysis to find the field distributions and effective indices, and derived their dependence from temperature as an effective thermo-optic coefficient,  $dn_{eff}/dT$ . Data results clearly show that appropriate thermo-optic structures with same polarization behaviour can be selected in order to optimize the effective thermo-optic effect in SOI rib waveguides. This is significantly different from the procedure followed in literature, where only the bulk thermo-optic coefficient is usually taken into account. It is to note that, in our modelling procedure, the heater thickness has not influence on thermal simulation results.

Finally, we have calculated the switching power and the cut-off frequency [13] following an approach similar to that presented in [14] using a Mach-Zehnder scheme, namely:

$$P_\pi = \lambda k_{SiO_2} (dn_{eff}/dT)^{-1} \left[ W / (2t_{SiO_2}) + \sqrt{k_{Si}/k_{SiO_2}} \sqrt{t \cdot h} / L \right] \quad (1)$$

where  $L = 1 \text{ mm}$  is the heater length and the term  $\sqrt{k_{Si}/k_{SiO_2}} \sqrt{t \cdot h}$  takes into account the heat laterally spread beyond the heater [14]. The other geometric symbols are all explained in Fig. 1. The cut-off frequency  $f_{cut-off}$  is directly related to the switching power [14] by:

$$f_{cut-off} = (P_\pi / \pi \lambda \rho C_{SiO_2} A) (dn_{eff}/dT) \quad (2)$$

where A denotes the heated area and has been calculated as

$$A = \left( 2\sqrt{k_{Si}/k_{SiO_2}} \sqrt{t \cdot h} + W \right) (h + R + H) \quad (3)$$

Through this equation the cut-off frequency for all the structures under investigation (see Tables 1, 2) has been determined. Their response time has been obtained as  $\tau = 1/(e \cdot f_{cut-off})$ . Moreover, the single-mode characteristic of these structures should allow high switch on-off ratio to be achieved [14].

Some remarks can be derived observing Table 1. By following a full 2D approach, the temperatures of the heater and the waveguide core are different from each other. This is particularly evident in our small structures. By reducing the distance  $H$  of the heater from the waveguide, the thermo-optic coefficient gets better, the switching power decreases and also the response time becomes faster. This behaviour is valid for all the waveguides we have examined. Figures 2(a) and 2(b) shows thermal distribution and effective refractive index change versus the heater temperature in the structures 1a ÷ 1e, i.e., in waveguides where only the distance  $H$  has been varied. The numbers in brackets designate the line slopes, i.e., the calculated effective thermo-optic coefficients  $dn_{eff}/dT$  of the structures.

Main parameters of thermo-optic phase shifters are strongly depending on the waveguide and heater width (see Figs. 3(a) and 3(b)). Observing the structures under investigation, it can be noted that switching power  $P_\pi$  decreases if the dimensions of the waveguides and heaters

are scaled down. Moreover,  $P_\pi$  shows unexpectedly slow dependence on the rib width if the heater width is constant ( $W = 3 \mu\text{m}$ ).

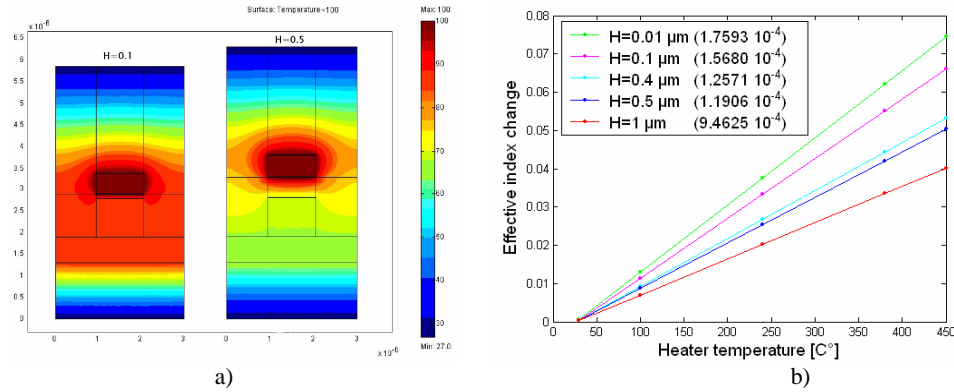


Fig. 2. (a) Thermal distribution at heater temperature of 100 °C and (b) effective refractive index change versus heater temperature for various distance  $H$  of the heater in structures of series 1.

In general, we have to use smaller waveguides to provide better switching characteristics ( $f_{\text{cut-off}}/P_\pi$  ratio), but at some expenses in decreased effective thermo-optic coefficient  $dn_{\text{eff}}/dT$ , especially if the waveguide dimensions are close to the fundamental mode cut-off. The trade-off between conflicting requirements occurs at rib widths ranging around  $1\div3 \mu\text{m}$ , providing optimum tuning rate at moderate power ( $6\div16 \text{ mW}$ ) and large cut-off frequency ( $2\div10 \text{ kHz}$ ). This opens the way to develop a new set of tuneable devices based on MR-filtering technology providing super-resolution (narrow linewidth), to be used in HDWDM fiber-optics networks.

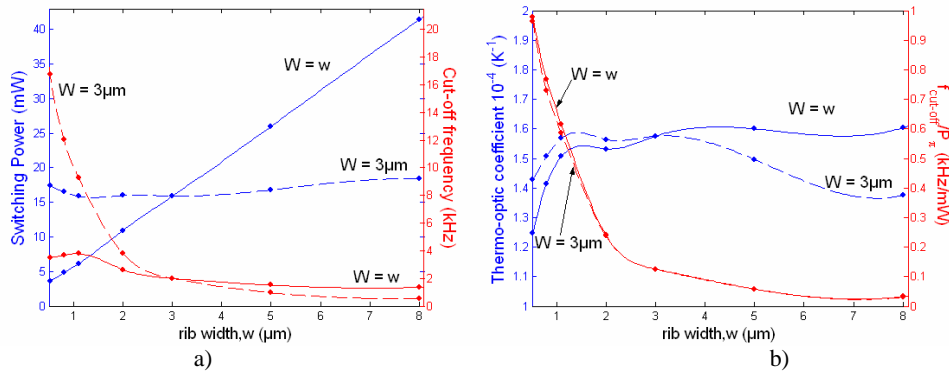


Fig. 3. (a)  $P_\pi$  and cut-off frequency, (b)  $dn_{\text{eff}}/dT$  and  $f_{\text{cut-off}}/P_\pi$  ratio, versus the waveguide rib width.

### 3. Multi-reflection filtering technology

Multi-reflection filtering technology [9] is based on the use of the multi-reflector beam expanders [10-11] and optical phase shifters. The principal scheme of multi-reflector ROADM with rib waveguide structures and thermo-optic phase shifters is shown in Fig. 4. It contains four multi-reflector beam expanders and a set of rib waveguides to guide partially reflected optical sub-beams. The work of MR-ROADM can be described as follows.

Input optical beam (In) passes through the first beam expander, based on the channel (rib) optical waveguide crossed by the multiple periodically spaced partial reflectors. Beam expander is working by splitting the input light into multiple sub-beams. Note that, differently from the principal scheme of Fig. 4, the real multi-reflector beam expander can contain multi-

hundreds partial reflectors that have small reflection coefficients and low scattering losses. Thus at every reflector the larger part of optical energy passes through the waveguide to the next reflector (and further split into two parts) and the smaller part is reflected. The reflected optical sub-beam (that turns the direction of propagation related to input one) crosses the small spacing between the waveguides and enter with low losses to another optical waveguide (slanted to the input one), containing optical phase shifting elements intended for wide tuning of optical wavelength. Then these reflected sub-beams come to the next beam expander of the Drop channel that works as a reciprocal optical element. Namely, every sub-beam crosses the small spacing between the waveguides and is split into two parts.

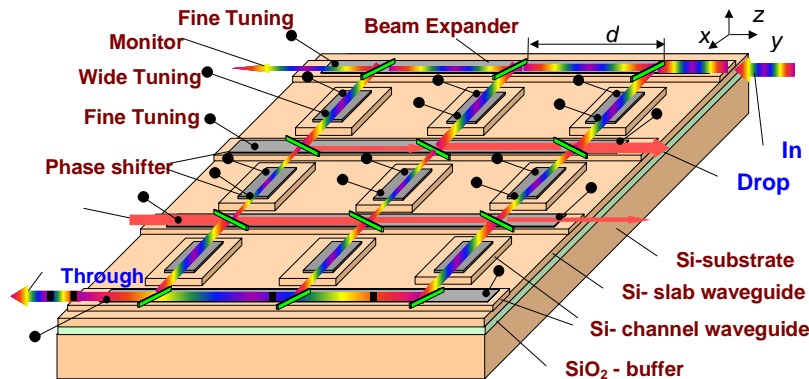


Fig. 4. Schematic diagram of the proposed type of MR-ROADM.

One part is reflected and directed along the optical waveguide of Drop channel, the other part is passed through the reflector to the next beam expander of the Add channel. The optical power that passes from device input to output has to be examined taking into account reflection and interference of multiple sub-beams. At every dropped frequency all sub-beams interfere in those manner that they add in phase along axis of Drop waveguide and thus provide high intensity of Drop signal due to the effect of constructive interference. At the same optical frequency, all sub-beams concise each other in the cross direction and thus only a small power is coming to the next waveguide (Add). At each other optical wavelength the condition of constructive interference is broken and optical sub-beams passes through the Drop beam expander with a small loss of energy, thus having a small signal to be dropped by the device. The beam expander of the Add waveguide has the same period and orientation of reflectors as the Drop one and both of them satisfy the same condition of constructive or destructive interference. Thus this beam expander can be used to add optical signal at the same (Drop) wavelength to the thought pass of the device and besides it increases suppression of the parasitic signal at the Drop wavelength that may be not fully filtered by the previous beam expander.

The last beam expander “Through” is manufacturing in the way similar to the first “In” beam expander, thus all sub-beams that come to its output are entered in phase and effectively transformed to the “Through” pass fiber. The device efficiency is optimized by the proper choice of the function  $R(M)$  of the reflection coefficient over the reflector number  $M$  of all beam expanders. Proper choice of the apodization function  $R(M)$  provides small contribution to multiple interference from the reflectors placed near the edges of the beam expanders and large contribution from the reflectors at the center part of the beam expander. In general, optimization procedure takes into account the desired frequency response of “Drop”, “Add” and “Through” signals, insertion losses, sidelobe suppression and optical crosstalk. For example, for the loss-less optimal case, device has internal loss of Drop and Through signals of only -0.1 dB. If we take into account the reasonable scattering losses (say 10% of energy

scattered at each reflector), then the internal losses of Drop and Through signals are increased up to -1.3 dB.

One can show [9] that device picks up (drops) only those optical wavelengths that satisfy the condition of constructive interference, depending of the parameters of the beam expander (angle and period of reflectors, as well as refractive index in the strip waveguide) and the refractive index, length and orientation of the waveguide array. The tuning of the filtered optical wavelength can be obtained by manufacturing optical phase shifting arrangement along the beam expanders (for fine-tuning) and along the waveguide array (for wide tuning). These optical phase shifters have to be tuned by temperature heaters in such a manner that it will provide linear phase shift over the number of optical sub-beams that pass through the waveguide array. Tuning of the device within the total free spectral range corresponds to  $2\pi$  phase change between neighbor sub-beams. Thus one can control the optical wavelength that corresponds to the condition of constructive interference and has to be effectively filtered or/and added by the device.

#### 4. FDTD simulations of MR-ROADM

MR-ROADM is the novel type of optical device that has not yet been studied experimentally. Here we present the first results of device simulation obtained by the finite difference time domain (FDTD) method [15], that can be regarded as a computer experiment. Here we have examined the multi-reflector beam expander technology in 2D case. Physically it corresponds to the situation when one of 3D dimensions is infinitive. Practically, it corresponds to 3D-waveguide structure with reflectors that overlap area of the guided mode in cross (Z) direction. The simulation design of MR-demultiplexer that contains three BE based on the strip waveguides with 10 partially reflected 45-degree slanted strips is shown in Fig. 5(a).

Results presented in Fig. 5(b) prove the general concept of MR-ROADM. It shows that ROADM has multiple reflection and transmission passbands corresponding to different order of constructive interference of sub-beams reflected from multiple reflection strips of beam expanders. General limitation of FDTD makes impossible to examine real devices that have too large dimensions. Nevertheless it helps us to determine phenomenological parameters as  $T = 0.83$ ,  $R = 0.15$ ,  $b = \alpha/R = 0.16$ , and  $\phi_T = 0.53$  that are used in the further analyze of real devices by home-made software, where  $R$  and  $T$  are reflection and transmission coefficients of the partial reflector, respectively,  $\alpha = 1 - R - T$  is the measure of scattering losses,  $\phi_T$  is the additional phase change in the transmitted light due to the presence of the partial reflector. Figure 5(b) has been obtained for a refractive index of the waveguide, surrounded media and refractive strip of 2.21, 2.205, and 1.9, respectively, waveguide width of  $5 \mu\text{m}$ , reflector strip depth and width of  $0.29 \mu\text{m}$  and  $9 \mu\text{m}$ , and period of reflectors of  $10 \mu\text{m}$ .

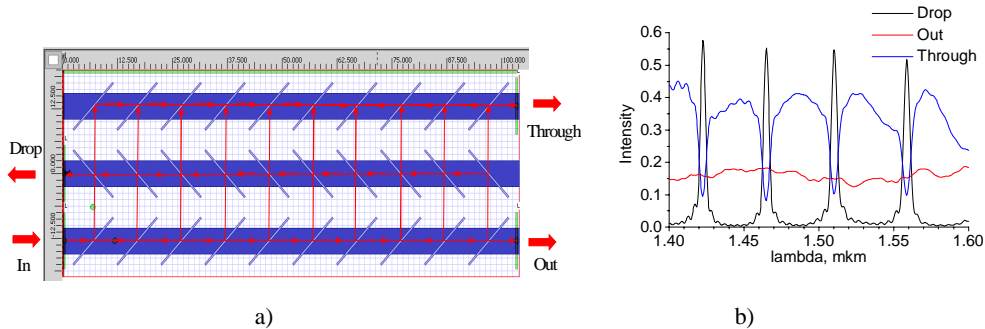


Fig. 5. (a) Design of MR-demultiplexer and (b) its frequency response simulated by 2D FDTD.



## 5. Simulations of MR-ROADM with thermo-optic tuning on SOI waveguides

Based on results of Sections 2-4, we present here the first examination of the prototype of MR-ROADM compatible with silicon-on-insulator (SOI) technology. SOI partial reflectors can be manufactured by etching deep grooves and filling them with a material having different optical properties, for example by growing polysilicon containing some part of oxygen (a-Si:H/SiO<sub>2</sub> [16]) or carbon (a-SiC:H [17]), to decrease the pure silicon refractive index. Technology of deep etching with filling is widely used for MEMS and Bragg reflectors.

Phase shifting elements are optimized according to the structure 1d shown in Table 1. This single-mode structure presents the important advantages to have a good thermo-optic effect and moderate switching power. Fine tuning arrangement is simple and reliable, as the filtered optical wavelength can be tuned by the single signal applied to the phase shifters incorporated along the beam expander. It is also to note that MR-ROADM with rectangular waveguide arrangements has similar tuning rates as ROADM based on conventional Bragg grating or ring architectures.

MR-ROADM tuning within a total FSR of 5 THz (i.e., 40 nm, that is a typical demand for DWDM working within C- or L- band) corresponds to  $2\pi$  optical phase between the adjusted strip waveguides. It needs unpractical changes of refractive index,  $\Delta N = 0.09$ , and temperature,  $\Delta T = 480$  °C in the SOI waveguide core. To eliminate this principal limitation, MR-ROADM utilizes wide tuning phase shifters, 1 mm long ( $\Delta N = 0.0008$  and  $\Delta T = 4.2$  °C). They could be individually tuned according to a folded-over module ( $2\pi$ ) scheme and arranged in groups (to decrease the number of controlling electric signals). Combination of "wide tuning" and "fine tuning" in the same device increases its flexibility, as one has to arrange tuning within the total FSR (desired C- or L-band) by small changes of refractive index, obtained through electrical signals applied to the appropriate phase shifters. For example, "wide tuning" can "digitally" tune ROADM by  $\text{FSR}/m_f$  steps, and any desired optical wavelength can be dropped by "fine tuning" arrangement covering only  $1/m_f$  part of FSR. Thus, fine tuning  $m_f$ -times smaller requires smaller refractive index/temperature change, as well as switching power.

High side-lobe suppression is obtained by the appropriate variation of BE reflector coefficients, as in Fig. 6(a). Typical frequency responses of 25 GHz MR-ROADM for different refractive index change in fine tuning waveguides are shown in Fig. 6(b). The device can be tuned within the total C- or L- band by means of wide tuning sections. Devices for any other ITU grid (12.5 GHz or 50 GHz) have similar characteristics (where the appropriate linewidth is an inverse function of the reflector number,  $N_r$ ). Parameters of typical MR-ROADMs intended for high dense ITU grids ( $G = 12.5 \div 50$  GHz) with multi-hundreds wavelength channels (#W.Ch.) are summarized in Table 3.

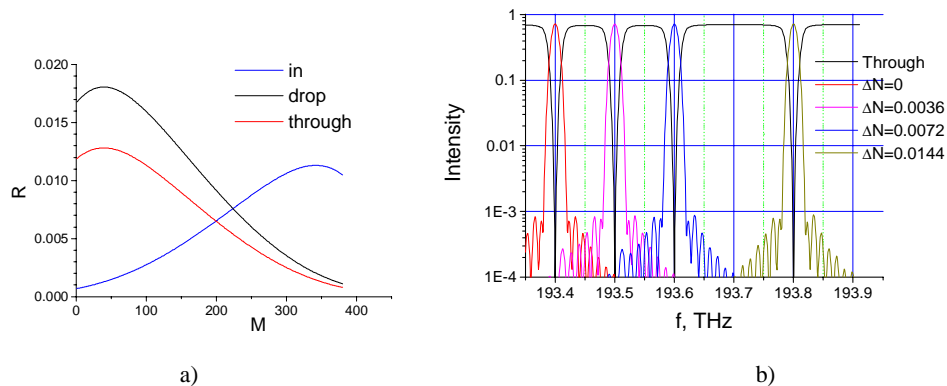


Fig. 6. (a) Reflector coefficients apodization for in, drop and through beam expanders and (b) simulated frequency response of 25 GHz ROADM.



Here  $P_f = N_r \cdot P_{\pi}$  and  $P_w = N_r \cdot P_{\pi}/2$  are the maximum powers, for tuning within a FSR of 5 THz, that can be applied to fine and wide tuning phase shifters, respectively. It holds  $P_{\pi} = 6.14$  mW, while  $P_{\pi} = 21.8$  mW is the switching power for fine tuning when  $L$  is equal to the period of reflectors,  $d = 8.64$   $\mu\text{m}$ . Sidelobe suppression and extinction ratio are better than -29 dB. Total losses for Drop and Through signals are -2.5 dB and -2.7 dB, respectively. We have also taken into account a number of loss sources, including internal ROADMs losses of 1.3 dB, waveguide losses of 0.2 dB/cm, waveguide crossing losses of 0.1 dB/cm and fiber coupling losses of 0.5 dB per facet.

It is known that reflected and transmitted light exhibits strong polarization dependence, especially for the case of a right angle orientation of beam expander and channel waveguide (see Fig. 5(a)), when the light is incident on the reflector array at tilting angle close to the Brewster one. Thus MR-ROADM is able to work with the quasi-TM polarized single mode.

To provide low polarization-dependent losses (PDL), one needs to use two identical single-polarization MR-ROADMs including polarization splitters and rotators. Namely, incident signal has to be split into two polarizations (TE and TM), TE polarization has to be rotated into TM polarization, and both of them have to be simultaneously filtered by two ROADMs. Then, two sets of drop/through signals will join together at the output of the device by the next polarization/splitter arrangement, that has a symmetrical architecture to obtain very low PDL.

Table 3. Parameters of typical MR-ROADM on SOI platform.

$G$ [GHz]	# W.Ch.	$N_r$	$P_f$ [W]	$P_w$ [W]	$L_r$ [cm]
50	100	190	4.14	0.58	0.164
25	200	380	8.27	1.17	0.33
12.5	400	760	16.55	2.34	0.66

## 6. Summary

The paper presents an investigation of thermo-optic phase shifters in silicon-on-insulator guided-wave structures and recommendations to provide high tuning characteristics at minimum power requirements, namely by reducing the heater distance from the waveguide core, choosing smaller waveguide and heater sizes. A combination of known technology of low-loss SOI optical waveguides, efficient thermo-optic phase shifting elements, and high aspect ratio etching and back filling of silicon with the multi-reflector patented technology provides the possibility of developing a novel type of tunable optical elements (TOF and ROADM) for HDWDM. Multi reflector filtering technology is based on constructive or destructive interference of multiple sub-beams that join together at the output of beam expanders, making possible to Drop any desired wavelength signal and to Add it to the pass Through output. Additional phase shifting elements for fine tuning (along the beam expanders) and wide tuning (along the waveguide array) produce a linear phase shift over the channel waveguide number and make the device fully reconfigurable over a large free spectral range, covering the whole C- or L- bands. Multi reflector filtering technology has a strong market perspective as it leaves behind simultaneously parameters of many competitive technologies in device size, number of tunable wavelength channels (up to 400) and linewidth (up to 6 GHz). It should give a new opportunity for developing super resolution, compact, tunable optical devices, and could be used with high dense ITU grids (50 GHz, 25 GHz, or 12.5 GHz), very promising for utilization in HDWDM flexible fiber optical networks.

## Acknowledgments

We would like to thank Institute of Semiconductor Physics (Novosibirsk, Russia), Russian Academy of Sciences, and company Gilad Photonics, Israel, that provided initial investment for studying MR filtering technology. We would like to thank Companies Optiwave Corporation and Comsol Inc for providing commercial softwares. Moreover, the authors wish to thank the paper referees for useful comments and suggestions.